Probing Vela Pulsar down to 20 GeV with H.E.S.S. II observations

A. Djannati-Ataï[1,a)], G. Giavitto[2], M. Holler[3], B. Rudak[4], C. Venter[5] and The H.E.S.S. Collaboration

[1]*APC, AstroParticule et Cosmologie, Université Paris Diderot, CNRS/IN2P3, CEA/Irfu, Observatoire de Paris, Sorbonne Paris Cité, 10, rue Alice Domon et Léonie Duquet, 75205 Paris Cedex 13, France*
[2]*DESY, D-15738 Zeuthen, Germany*
[3]*Laboratoire Leprince-Ringuet, Ecole Polytechnique, CNRS/IN2P3, F-91128 Palaiseau, France*
[4]*Nicolaus Copernicus Astronomical Center, ul. Bartycka 18, 00-716 Warsaw, Poland*
[5]*Centre for Space Research, North-West University, Potchefstroom 2520, South Africa*

[a)]Corresponding author: djannati@in2p3.fr

Abstract. Observations of the Vela pulsar (PSR B0833−45) with the High Energy Stereoscopic System phase II array (H.E.S.S. II) have resulted in a high-significance detection of its pulsed emission down to 20 GeV. The very low-energy threshold reconstruction and analysis methods developed specifically for the monoscopic mode are presented together with detailed comparison of the results obtained with five years of *Fermi*-LAT data. A very good agreement is obtained between the two instruments, thereby validating the overall analysis chain and the response model of the largest H.E.S.S. telescope (CT5). The high event statistics are used to probe the spectrum of PSR B0833−45 above 20 GeV.

Introduction

The H.E.S.S. array of imaging atmospheric Cherenkov telescopes (IACTs), located in the Khomas Highland of Namibia (1800 m), was upgraded in 2012 with the addition of a 28 m equivalent diameter telescope (CT5) to its core array of four 12 m diameter telescopes (CT1-4). The aim of this upgrade, referred to as H.E.S.S. II, is to bridge the gap with satellite-based γ-ray instruments by pushing the energy threshold of the array from above 100 GeV to below the standard analysis threshold. In order to attain the lowest possible threshold, the trigger system of the initial array was modified such as to keep events where CT5 triggers, regardless of the state of other smaller telescopes. For those events, referred to as monoscopic, a new reconstruction technique has been developed. The Vela pulsar, PSR B0833−45, i.e. the brightest pulsar in the GeV sky, was one of the prime targets in the commissioning period of H.E.S.S. II, during which 24 h of good quality data at zeinth angles smaller than 40° was taken (data set I, below). The second peak of PSR B0833−45, P2, was subsequently detected with an excess count of 9789 events, at a significance level greater than 12 σ when using a simple likelihood ratio test [10] within the predefined phase range [0.5-0.6], and of 15.2 σ when evaluated with the H-test [6].

To probe the performance of CT5 near its detection threshold energy, results from this data set were compared to expectations from detailed Monte Carlo (MC) simulations of the instrument, for which the γ-ray spectrum above 10 GeV of PSR B0833−45 was used as input signal. This spectrum was obtained from analysis of 5 years of *Fermi*-LAT data. In a second step, an additional data set of 16.3 h from normal operations (data set II) was added to the commissioning data to study the phase profile and the spectrum of the Vela pulsar in the H.E.S.S. II and *Fermi*-LAT overlapping energy range. The overall excess for the whole data set (40.3 h) amounts to 15835 events, corresponding to a significance level of 15.6 σ (17.9 σ with H-test). The lightcurves obtained from the two instruments are shown on Fig. 1.

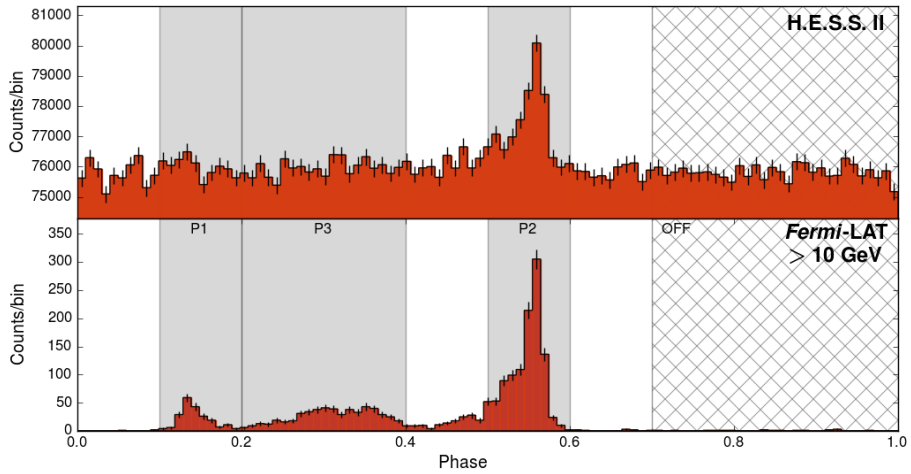

FIGURE 1: PSR B0833−45 phasogram obtained using 40.3 h of H.E.S.S. II data and 60 months of *Fermi*-LAT data. *On*-phase intervals for P1, P2 and P3 are shown in gray; the *Off*-phase interval is shown as a hatched area. To compute the pulsar phase, selected events were folded using the `Tempo2` *Fermi* plugin, ephemerides provided by LAT Gamma-ray Pulsar Timing Models [12] covering *Fermi*-LAT and H.E.S.S. II observations.

H.E.S.S. II monoscopic data analysis

An event-based reconstruction pipeline, aiming at the lowest threshold energy, was developed to estimate the shower direction, impact distance and energy. The shower reconstruction algorithm assumes that its direction lies on the major axis of the image and that, for point-like source of known position, e.g. pulsars, it points toward the inner part of the camera. MC-based studies have shown that this provides a better angular resolution at the lowest energies, at the expense of a slightly higher background. Finally, the direction is derived using an estimate of the angular distance of the image barycenter to the source position, δ, which is obtained thanks to a Neural Network (NN) based on the image length, λ, width, ω, and charge, Q. The shower impact distance, ρ, and energy estimators rely also on NNs using image parameters. To avoid the smearing of the energy estimator by the impact distance error, the true value, ρ_{true}, is used during the NN training process. The event direction reconstruction achieves a Point Spread Function (PSF) of 68% containment radius $R_{68} = 0.3^\circ$, when evaluated for a power law of index $\Gamma = 2.0$ in the range from 5 to 120 GeV, at 20° zenith angle. The PSF does not vary much with the index, e.g., $R_{68} = 0.32^\circ$ for $\Gamma = 4.0$. The energy estimator has a large bias near the threshold, e.g., 50% at 20 GeV, but improves with increasing energy (see Fig. 2). The integrated dispersion for a power-law of index $\Gamma = 2.0$ is $\ln(E_{\rm rec}/E_{\rm true}) = 43\%$ with a bias of $\sim 3\%$. The performance for a steeper spectrum of $\Gamma = 4.0$ degrades to 50% and 41% for the dispersion and bias, respectively.

To reject the background, in addition to the spatial cut on the reconstructed angle of the events with respect to the source position, a Boosted Decision Tree (BDT) classifier[1], in the same spirit as that for the H.E.S.S. I array [5], is used. The input parameters of the classifier consist of the above-mentioned image shape parameters, λ and ω, together with additional physical parameters of the shower, i.e. the maximum depth in the atmosphere, length and width, obtained from a 3D Gaussian-model fit of the its photosphere [9]. The analysis cuts were optimized to yield a large effective area near threshold, e.g., 4.5×10^3 m^2 at 20 GeV (see Fig. 2), at the cost of a reduced γ-background separation. A total charge cut $Q_{\rm min} = 30$ p.e. and a BDT discrimination value of $\zeta = -0.1$ result in a background rejection factor of 70%, while keeping 95% of the signal. Further separation power is obtained through a selection in pulsar phase, with intervals defined a priori using the *Fermi*-LAT light curve (see Fig. 1). An alternative analysis pipeline, using a different approach based on a semi-analytical model of electromagnetic particle showers in the atmosphere [7], was used to cross-check the results reported here on the signal and the phasogram, and yielded consistent results.

[1] Based on the TMVA package [8].

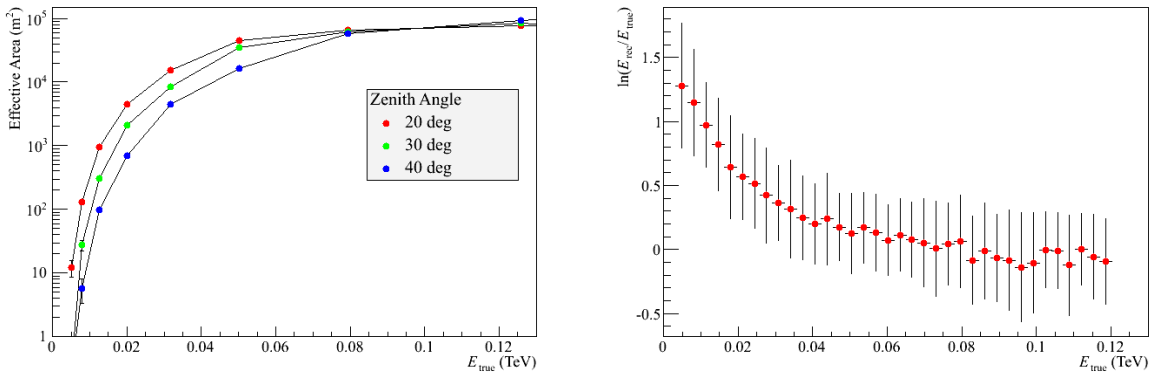

FIGURE 2: *Left:* Effective area as a function of energy for different zenith angles: the specific analysis used here has been developed to yield a large effective area near threshold, i.e. 4.5×10^3 m^2 at 20 GeV and 20° zenith angle. One notes the rapid increase of the threshold energy as a function of zenith angle, e.g. a drop in area of a factor of ~ 10 below 30 GeV when comparing the 40° and 20° zenith angles. *Right:* Distribution of $\ln(E_{\rm rec}/E_{\rm true})$ as a function of $E_{\rm true}$ at 20 deg zenith for a power-law distribution between 5 and 120 GeV with index $\Gamma = 2$. Error bars show the spread (RMS) of events around the average value. Note that bins are correlated.

Commissioning of CT5 using the Vela pulsar as test-beam

The spectrum of the pulsar's P2 peak above 10 GeV was input to extensive MC simulations of CT5 in order to derive the expected signal from H.E.S.S. II data set I and check the instrument response model. The spectrum was derived thanks to 60 months of *Fermi*-LAT data, from August 4, 2008, to July 26, 2013, using `P8` Source class events and `P8R2_SOURCE_V6` Instrument Response Functions (IRFs). A simple power law fit to the data resulted in an spectral index of $\Gamma = 4.1 \pm 0.1^{\rm stat} \pm 0.05^{\rm sys}$ with normalisation $\Phi_0 = 4.1 \pm 0.2^{\rm stat} \pm 0.3^{\rm sys} \times 10^{-8}$ TeV^{-1}cm^{-2} s^{-1}, at a reference energy $E_0 = 25$ GeV (see Fig. 4). Testing the *Fermi*-LAT data for curvature above 10 GeV with a log-parabola model yielded a 2.7σ preference for curvature. A simple power-law model was hence considered as best describing the P2 spectrum in the energy range overlapping with H.E.S.S. II, independent from the lower-energy part of the emission. This resulted in a MC expected number of γ-ray events for H.E.S.S. II of $N_{\rm MC} = 11697 \pm 675$, in good agreement with the measured excess, $N_{\rm exp} = 9789 \pm 787$. Although the deviation of 1908 ± 1037 events, corresponding to a ratio $\eta = N_{\rm exp}/N_{\rm MC} = 0.84 \pm 0.08$, is of low statistical significance ($\lesssim 2\sigma$), it might point to systematic errors in the CT5 effective area and/or a difference between the energy scales of the two instruments. Figure 3 shows the comparison of the reconstructed angle (θ^2, *left*) and energy distributions (*right*) between data and MC simulations. The latter have been weighted so as to represent the power law fitted to the *Fermi*-LAT data and scaled to correct for η. When investigating the simulated true-energy distribution (shown in blue on Fig. 3, right panel), a significant overlap in energy range can be inferred between H.E.S.S. II in monoscopic mode and *Fermi*-LAT. Indeed this distribution peaks at 20 GeV with more than 40% of events lying below this energy. The agreement between the real and simulated distributions validates the overall analysis pipeline and the MC model of the instrument response down to its threshold.

P2 Energy spectrum above 20 GeV

The energy spectrum of P2 was subsequently derived with the H.E.S.S. II data above an energy of 20 GeV. The spectrum reconstruction pipeline is based on a forward-folding maximum likelihood fitting procedure for *a priori* chosen spectral models [11]. It was validated by reconstruction of 150 MC-generated power-law spectra with index $\Gamma = 4.0$, where background events were included with a signal-to-noise ratio similar to that of the real data.

The fit of a simple power law in the energy range 20-110 GeV results in an index of $\Gamma_{\rm HESS} = 4.1 \pm 0.2^{\rm stat} \pm 0.2^{\rm sys}$, and a normalisation $\Phi_0^{\rm HESS} = 3.1 \pm 0.2^{\rm stat} \pm 0.9^{\rm sys} \times 10^{-8}$ TeV^{-1}cm^{-2} s^{-1} at a reference energy $E_0 = 25$ GeV (see Table 1 and Fig. 4). Using a log-parabola model in order to test for curvature in the spectrum only marginally improves the fit ($\lesssim 1\sigma$). The last significant bin, in the 92-110 GeV *reconstructed* energy range, exhibits an excess of 986 events

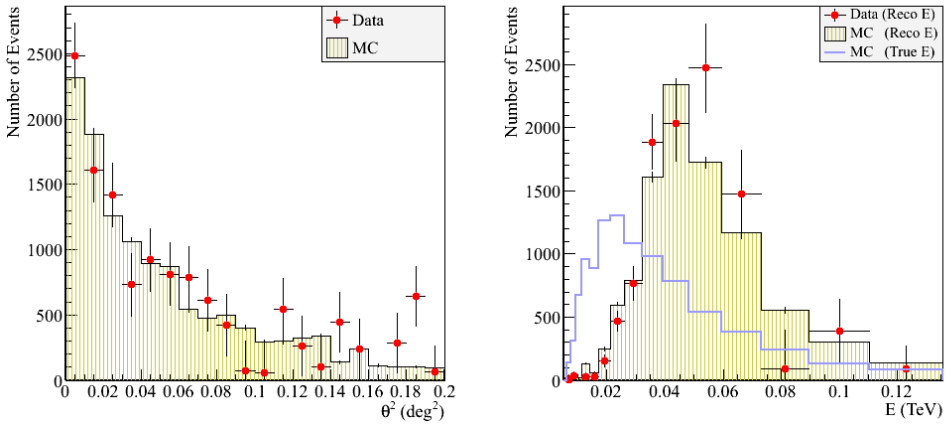

FIGURE 3: Comparison of the reconstructed angle (θ^2, *left*) and energy distributions (*right*) between data and MC simulations. The light blue curve on the right panel is the corresponding MC-generated energy distribution for selected events, and peaks slightly above 20 GeV: $\sim$ 40% of events lie below this energy. Note that the energy distribution histogram bin widths are defined in logarithmic scale.

at a significant level of 3.1 σ. The average true energy of events in this bin is $\bar{E}$ = 75 GeV with an RMS of 32 GeV, due to the migration of events from lower energy bins (given the large bias in the energy reconstruction, see Fig. 2, right panel). Systematic errors on the spectral parameters were investigated by fitting data sets I and II independently, as well as other subdivisions of data. Further investigations included the use of an alternative atmospheric extinction model and different threshold and maximum energies for the fitting process. These studies have shown the best-fit values to remain stable at better than ±30% for the flux and ±0.2 for the spectral index. As compared to the vaues obtained for the *Fermi*-LAT above 10 GeV, results are in an excellent agreement for the spectral index, with a flux normalisation ratio of $\Phi_0^{\rm HESS}/\Phi_0^{\rm LAT} = 0.76 \pm 0.07^{\rm stat} \pm 0.22^{\rm sys}$ (see Fig. 4), which is compatible with unity given the systematic uncertainties.

Conclusions

Using 40.3 h of observations with the H.E.S.S. II largest telescope, pulsed emission has been detected from the P2 peak of PSR B0833−45 at a significance greater than 15 σ. The very good agreement obtained between data and MC-generated distributions has validated the very low-threshold analysis and the numerical response model of the CT5

TABLE 1: Vela pulsar P2 spectrum best-fit parameters for a power law in the range 20-110 GeV for data sets I and II, the overall data set using two atmospheric extinction models. The values obtained for *Fermi*-LAT data above 10 GeV are shown for comparison. Systematic errors are discussed in the text.

Instrument	**Data set**	**Extinction**	$\mathbf{\Phi_0}^*$	$\mathbf{\Gamma}$
H.E.S.S. II	I	standard	3.1 ± 0.3	4.1 ± 0.3
H.E.S.S. II	II	standard	2.9 ± 0.3	3.9 ± 0.3
H.E.S.S. II	total	standard	3.1 ± 0.2	4.1 ± 0.2
H.E.S.S. II	total	alternative	3.4 ± 0.5	4.1 ± 0.2
Fermi -LAT	60 months	-	4.1 ± 0.2	4.1 ± 0.10

* In units of 10^{-8}TeV^{-1}cm^{-2} s^{-1} at the reference energy E_0 = 25 GeV.

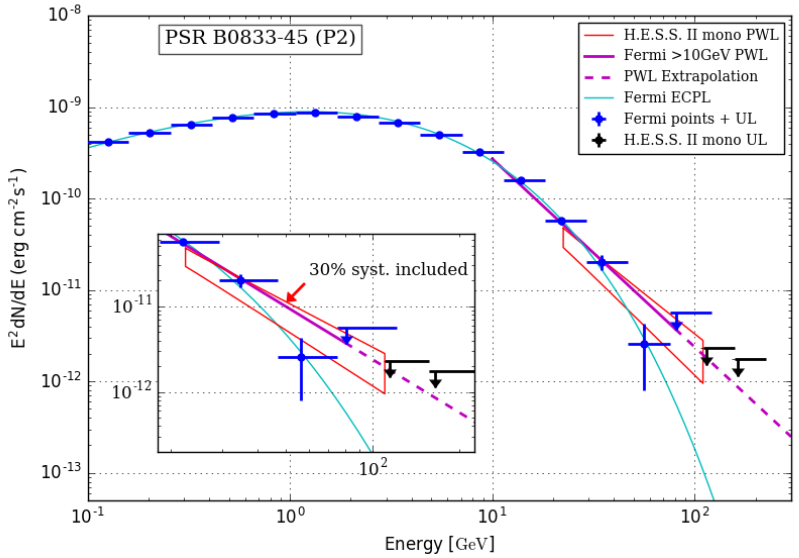

FIGURE 4: Spectral energy distribution of the P2 peak of PSR B0833−45. The red butterfly shows the confidence interval for the power-law fit to H.E.S.S. II data in the 20-110 GeV energy range where the statistical (1 σ) uncertainty box has been extended such as to include a ±30% systematic error on flux. The power-law fit to the *Fermi*-LAT data above 10 GeV is shown in solid magenta with a dashed line for its extrapolation above 80 GeV. The blue line indicates the result of the fit of a power law with an exponential cutoff in the range 100 MeV to 120 GeV. *Fermi*-LAT flux points and upper limit are given in blue, and 99.7% upper limits derived from H.E.S.S. II data are shown in black.

telescope down to its threshold. It was shown that more than 40% of selected events lie below 20 GeV in true energy units, an unprecedented low energy for ground-based γ-ray astronomy. The fit of a power law to the H.E.S.S. II energy spectrum of P2 yields a steep index of $\Gamma_{\rm HESS} = 4.1$, very consistent with that obtained from 60 months of *Fermi*-LAT data above 10 GeV. In addition, the H.E.S.S. II to *Fermi*-LAT flux ratio $\Phi_0^{\rm HESS}/\Phi_0^{\rm LAT} = 0.76 \pm 0.07^{\rm stat} \pm 0.22^{\rm sys}$ is compatible with unity given the systematic uncertainties.

Pulsar measurements with *Fermi*-LAT have shown strong flux attenuation for almost all γ-ray pulsars at energies higher than a few GeV. The discovery of pulsed Very High Energy (VHE; $\gtrsim$ 100 GeV) emission from the Crab pulsar, detected by the MAGIC and VERITAS collaborations [3, 1, 13, 2] up to energies of $\simeq$ 400 GeV, and recently extended to 1.5 TeV [4] is an exceptional case within this context and strongly challenges the current pulsar emission models. In the case of the Vela pulsar, while the *Fermi*-LAT spectral analysis of P2 above 10 GeV, independent of the lower-energy part, yields a 2.7σ preference for curvature, there is no significant indication for a deviation from the power law in the H.E.S.S. II data. However, given the current range of uncertainty (see Fig. 4), the spectrum remains consistent with both power-law and sub-exponential cutoff models. Deeper observations of PSR B0833−45 and other pulsars are needed to answer the important question of whether other pulsars might exhibit pulsed emission above 100 GeV.

Acknowledgments

The support of the Namibian authorities and of the University of Namibia in facilitating the construction and operation of H.E.S.S. is gratefully acknowledged, as is the support by the German Ministry for Education and Research (BMBF), the Max Planck Society, the German Research Foundation (DFG), the French Ministry for Research, the CNRS-IN2P3 and the Astroparticle Interdisciplinary Programme of the CNRS, the U.K. Science and Technology Facilities Council (STFC), the IPNP of the Charles University, the Czech Science Foundation, the Polish Ministry of Science and Higher Education, the South African Department of Science and Technology and National Research Foundation, the University of Namibia, the Innsbruck University, the Austrian Science Fund (FWF), and the Austrian Federal Ministry for Science, Research and Economy, and by the University of Adelaide and the Australian Research Council.

We appreciate the excellent work of the technical support staff in Berlin, Durham, Hamburg, Heidelberg, Palaiseau, Paris, Saclay, and in Namibia in the construction and operation of the equipment. This work benefited from services provided by the H.E.S.S. Virtual Organisation, supported by the national resource providers of the EGI Federation.

REFERENCES

[1] Aleksić, J., Alvarez, E. A., Antonelli, L. A., et al. 2011, ApJ, 742, 43
[2] Aleksić, J., Alvarez, E. A., Antonelli, L. A., et al. 2012, A&A, 540, A69
[3] Aliu, E., Anderhub, H., Antonelli, L. A., et al. 2008, Science, 322, 1221
[4] Ansoldi, S., Antonelli, L. A., Antoranz, P., et al. 2016, A&A, 585, A133
[5] Becherini, Y., Djannati-Ataï, A., Marandon, V., Punch, M., & Pita, S. 2011, Astroparticle Physics, 34, 858
[6] de Jager, O. C., Raubenheimer, B. C., & Swanepoel, J. W. H. 1989, A&A, 221, 180
[7] de Naurois, M. & Rolland, L. 2009, Astroparticle Physics, 32, 231
[8] Hoecker, A., Speckmayer, P., Stelzer, J., et al. 2007, PoS, ACAT, 040
[9] Lemoine-Goumard, M., Degrange, B., & Tluczykont, M. 2006, Astroparticle Physics, 25, 195
[10] Li, T.-P. & Ma, Y.-Q. 1983, ApJ, 272, 317
[11] Piron, F., Djannati-Atai, A., Punch, M., et al. 2001, A&A, 374, 895
[12] Ray, P. S., Kerr, M., Parent, D., et al. 2011, ApJS, 194, 17
[13] VERITAS Collaboration, Aliu, E., Arlen, T., et al. 2011, Science, 334, 69